AUV Real-time Dynamic Obstacle Avoidance Strategy Based on Relative Motion

Chongyang Lv, Fei Yu*, Minghong Zhu*, and Shu Xiao

***Abstract*—Based on the background of AUV path planning, the trajectory of dynamic obstacle is predicted according to the complex and changeable underwater environment and the motion characteristic of underwater vehicle which is different from mobile robot. AUV real-time obstacle avoidance strategy of the relative motion model is proposed in this paper. To achieve safe obstacle avoidance, we determine the probability of collision by analyzing the current location and movement condition of the vehicle and obstacles. We also adjust relative motion by changing the speed and direction of the vehicle. Finally, it can be proved by computer simulation experiment that this method can predict the trajectory of obstacles accurately, and make the vehicle avoid moving obstacles effectively so that to complete the planning of collision avoidance.**

***Index Terms*—autonomous underwater vehicles (AUV), relative motion, avoidance strategy, dynamic obstacle, EKF(Extended Kalman Filter), autonomous underwater vehicle navigation.**

I. Introduction

THE real-time obstacle avoidance of autonomous underwater vehicle (AUV) is the key to the safe navigation. The intelligent navigation is not only crucial for the AUV to successfully complete the scheduled task, but also important for AUV's own safety. In order to realize intelligent navigation, AUV should be able to avoid obstacles in the complex underwater environment with dynamic and static obstacles, and navigate safely through the target area to accomplish the tasks.

Many research groups have studied the dynamic path planning of AUV in dynamic obstacle environment, and proposed various solutions. The artificial potential field method is one of the most common methods for robot dynamic path planning. S. S.GE et al. [1]. suggested adding relative rate parameters to improve the algorithm in the traditional artificial potential field algorithm and achieved fairly good results. For robot obstacle avoidance in complex dynamic environment, Shiller et al. [2]. proposed a speed obstacle method through the combination of graphics technology and optimal method. Borenstein et al. [3] applied the vector field histogram method (VFH*, VFH+) for the real-time dynamic robot path planning problem. Fernandez[4] proposed a beam curvature method (BCM). The motion space of the robot is divided into several sectors. The obstacle avoidance in the robot dynamic environment space is implemented through calculating the speed solution of the optimal sector. Most of these methods are applied to the dynamic obstacle avoidance of mobile robot. However, there are great differences between the real-world underwater environment and the mobile robot environment. Moreover, the motion characteristics of underwater vehicles are different from those of mobile robots. Underwater vehicles cannot take sharp turns and abrupt stops like land robot, so the reaction is delayed. In view of the above situation, the relationship between the relative velocity and position was used to evaluate the possibility of collision in this article. Then the relative speed can be adjusted to avoid the obstacle by changing the size and direction of the submersible speed[5].

Manuscript received September 20, 2017; revised January 8, 2019. This work was supported by the National Natural Science Foundation of China under Grant No. 51679047.

C. Y. Lv is with the College of Science, Harbin University of Science and Technology, Harbin, P.R.China.

F. Yu (Corresponding author) is with the College of Automation, Harbin Engineering University, Harbin, P.R.China (e-mail: yufei@hrbeu.edu.cn).

M. H. Zhu (Corresponding author) is with the College of Automation, Harbin Engineering University, Harbin, P.R.China (e-mail: zhuminghong@hrbeu.edu.cn).

S. Xiao is with the College of Automation, Harbin Engineering University, Harbin, P.R.China.

II. Modeling of dynamic obstacles

In order to predict the motion of obstacles more accurately, it is necessary to select a motion model that is best suited for the target obstacles. The appropriate obstacle motion model is an important presumption to improve the prediction accuracy. The most common model used to match the motion of an underwater obstacle is the constant velocity model (CV model)[6] and the constant acceleration model (CA model)[6].

A. System modelling

In order to estimate the relative position and dynamics of the moving obstacle relative to AUV, we try to establish the extended Kalman filter.

The dynamic model of AUV is shown as

$$\mathbf{x}_{UUV}(k+1) = f(\mathbf{x}_{UUV}(k), n(k)) \tag{1}$$

Its discrete description can be shown as

$$\begin{bmatrix} x \\ y \\ z \\ \psi \\ u \\ v \\ w \\ r \end{bmatrix}_{(k+1)} = \begin{bmatrix} x + (uT + n_u\frac{T^2}{2})\cos\psi - (vT + n_v\frac{T^2}{2})\sin\psi \\ y + (uT + n_u\frac{T^2}{2})\sin\psi + (vT + n_v\frac{T^2}{2})\cos\psi \\ z + wT + n_w\frac{T^2}{2} \\ \psi + rT + n_r\frac{T^2}{2} \\ u + n_uT \\ v + n_vT \\ w + n_wT \\ r + n_rT \end{bmatrix}_{(k)} \tag{2}$$

where T represents the sampling time, $[x, y, z, \psi]$ represents the position and heading angle of AUV; $[u, v, w, r]$ represents the velocity and heading angle rate of AUV; $n = [n_u, n_v, n_w, n_r]$ represents the Gaussian noise of the velocity and heading angle rate.

B. Constant Velocity Model

When simulating obstacles, the simplest state of motion is a uniform linear motion. Constant velocity model (CV model)[6] is used in this case. Acceleration is zero when a body moves in a uniform linear motion, namely $\ddot{x}(t) = 0$. However, objects with uniform rectilinear motion are not possible in real world environments. Its motion must be subject to environmental disturbance, and its speed will change slightly. In this scenario, the change of acceleration is described as stochastic disturbance input. Simulations are performed using continuous white noise $\tilde{\omega}(t)$ in the model, supposing that the obstacle acceleration disturbance input is a Gauss distribution with zero mean, i.e.

We consider the obstacle moves with a constant speed its dynamic model will be shown as

$$\begin{bmatrix} x_o \\ y_o \\ z_o \\ v_{ox} \\ v_{oy} \\ v_{oz} \end{bmatrix}_{(k+1)} = \begin{bmatrix} x_o + v_{ox}T \\ y_o + v_{oy}T \\ z_o + v_{oz}T \\ v_{ox} \\ v_{oy} \\ v_{oz} \end{bmatrix}_{(k)} \tag{3}$$

where $[x_o, y_o, z_o]$ represents the position of the obstacle; $[v_{ox}, v_{oy}, v_{oz}]$ represents the velocity of the obstacle.

$$\ddot{x}(t) = \tilde{\omega}(t) \tag{4}$$

where

$$E[\tilde{\omega}(t)] = 0 \tag{5}$$

$$E[\tilde{\omega}(t)\tilde{\omega}^T(\tau)] = q(t)\delta(t-\tau) \tag{6}$$

The state vector corresponding to Eq. (1) is given as follows:

$$X(t) = \begin{bmatrix} x(t) \\ \dot{x}(t) \end{bmatrix} \tag{7}$$

The state equation of the obstacle is given as follows (sample interval is T):

$$X(k+1) = FX(k) + \omega(k) \tag{8}$$

wherein

$$F = e^{AT} = \begin{bmatrix} 1 & T \\ 0 & 1 \end{bmatrix} \tag{9}$$

The process noise is described as follows:

$$\omega(k) = \int_0^T e^{A(T-\tau)} \begin{bmatrix} 0 \\ 1 \end{bmatrix} \tilde{\omega}(kT+\tau)d\tau \tag{10}$$

C. Constant Acceleration Model

Another simple model for describing the motion of obstacles is constant acceleration model[6] (CA model). When the obstacle is uniformly accelerated, its jerk is zero, that is $\dddot{x}(t) = 0$. However, the acceleration of the obstacle can not be constant in practice. Therefore, the zero mean white noise can be used to describe jerks of the obstacle in the model.

$$\dddot{x}(t) = \tilde{\omega}(t) \tag{11}$$

The smaller the variance of $\tilde{\omega}(t)$ is, the more stable the acceleration is. The state vector corresponding to Eq. (8) is given in Eq. (9):

$$X(t) = \begin{bmatrix} x(t) \\ \dot{x}(t) \\ \ddot{x}(t) \end{bmatrix} \tag{12}$$

The discrete-time state equations with sampling intervals are the same as Eq. (5), wherein

$$F = e^{AT} = \begin{bmatrix} 1 & T & T^2/2 \\ 0 & 1 & T \\ 0 & 0 & 1 \end{bmatrix} \tag{13}$$

The covariance matrix of discrete process noise $\omega(k)$ can be listed in Eq. (11):

$$\begin{aligned} Q &= E[\omega(k)\omega^T(k)] \\ &= \begin{bmatrix} T^5/20 & T^4/8 & T^3/6 \\ T^4/8 & T^3/3 & T^2/2 \\ T^3/6 & T^2/2 & T \end{bmatrix} q \end{aligned} \tag{14}$$

Within the sample interval T, the jerk is approximately represented by $\sqrt{Q_{33}} = \sqrt{qt}$, which is the standard for a selected q.

D. Observation modelling

If the obstacle appears in the field-of-view of AUV, the relative range and bearing angle be measured. The observation model is shown as

$$\mathbf{z} = \begin{bmatrix} l \\ \theta \end{bmatrix} = \begin{bmatrix} \sqrt{(x-x_o)^2 + (y-y_o)^2 + (z-z_o)^2} \\ \arctan(\frac{y-y_o}{x-x_o}) - \psi \end{bmatrix} \tag{15}$$

E. EKF establishment

The extended kalman filtering is the most typical method to solve the optimal nonlinear filtering problem. As it is well known, the algorithm is based on the linearization of nonlinear system around the state estimate using the first-order Taylor expansion. The EKF implementation includes two steps: prediction and correction. Assuming that the initial state estimation is $\hat{\mathbf{x}}(0)$ and covariance is $\mathbf{P}(0)$, the prediction from time t_{k-1} to t_k can be conducted according to

$$\hat{\mathbf{x}}^-(k) = \mathbf{f}(\hat{\mathbf{x}}(k-1), \mathbf{u}(k-1), 0) \tag{16}$$

$$\begin{aligned} \mathbf{P}^-(k) = &\mathbf{F}(k-1)\mathbf{P}(k-1)\mathbf{F}^T(k-1) \\ &+\mathbf{G}(k-1)\mathbf{Q}(k-1)\mathbf{G}^T(k-1) \end{aligned} \tag{17}$$

where the superscript $-$ denotes the prediction of estimated state and covariance at time t_k, and the Jacobian matrix $\mathbf{F}(k-1)$ and $\mathbf{G}(k-1)$ can be obtained by:

$$\mathbf{F}(k-1) = \frac{\partial \mathbf{f}(\mathbf{x}(t), \mathbf{u}(k-1), 0)}{\partial \mathbf{x}}|_{\hat{\mathbf{x}}(k-1)} \tag{18}$$

$$\mathbf{G}(k-1) = \frac{\partial \mathbf{f}(\hat{\mathbf{x}}(k-1), \mathbf{u}(k-1), \mathbf{w}(t))}{\partial \mathbf{w}}|_{\bar{\mathbf{w}}(t)} \tag{19}$$

When the prediction step is finished, the estimated state and covariance at time t_k can be corrected based on the measurement $\tilde{\mathbf{z}}(k)$ using

$$\hat{\mathbf{x}}(k) = \hat{\mathbf{x}}^-(k) + \mathbf{K}(k)(\tilde{\mathbf{z}}(k) - \mathbf{h}(\hat{\mathbf{x}}^-(k))) \tag{20}$$

$$\mathbf{P}(k) = (\mathbf{I} - \mathbf{K}(k)\mathbf{H}(k))\mathbf{P}^-(k) \tag{21}$$

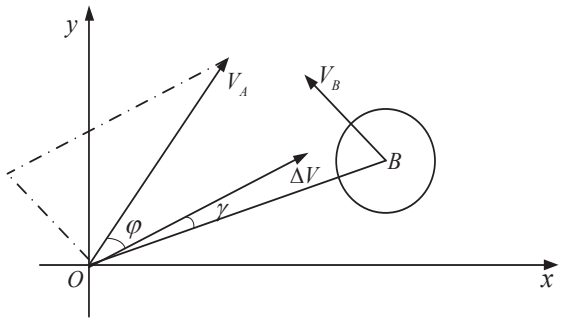

Fig. 1. Relative velocity diagram

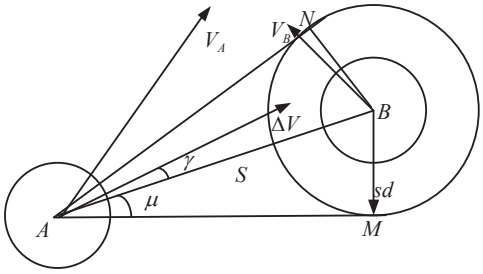

Fig. 2. Collision prediction model

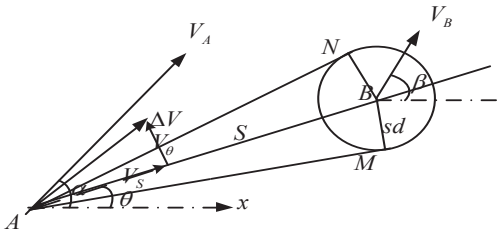

Fig. 3. Relation model between AUV and obstacle

where the kalman filter gain $\mathbf{K}(k)$ is computed by

$$\mathbf{K}(k) = \mathbf{P}^{-}(k)\mathbf{H}^{T}(k)(\mathbf{H}(k)\mathbf{P}^{-}(k)\mathbf{H}^{T}(k) + \mathbf{R})^{-1} \quad (22)$$

The sensitivity matrix $\mathbf{H}(k)$ can be calculated by

$$\mathbf{H}(k) = \frac{\partial \mathbf{h}(\mathbf{x}(t))}{\partial \mathbf{x}}|_{\hat{\mathbf{x}}^{-}(k)} \quad (23)$$

III. Collision Prediction and Collision Avoidance Strategies

A. Collision Prediction

The cruising velocity of an underwater vehicle at a fixed coordinate is $\mathbf{V_A}$. The position data of an obstacle returned by sonar is analyzed. And the Kalman filter is used to calculate the velocity $\mathbf{V_B}$ of the obstacle B in the fixed coordinate system. Using the obstacle as a reference, the velocity of underwater vehicle relative to the moving obstacle is given as follows:

$$\mathbf{\Delta V} = \mathbf{V_A} - \mathbf{V_B} \quad (24)$$

As shown in Fig. 1, O represents an underwater vehicle, and B represents a moving obstacle in space. $\mathbf{V_A}$ is the crusing velocity of the underwater vehicle. $\mathbf{V_B}$ is the velocity of the obstacle. $\mathbf{\Delta V}$ is the relative velocity. γ is the angle between the relative velocity direction and the line connecting the underwater vehicle and the moving obstacle. φ is the angle between the sailing velocity vector of the underwater vehicle and the relative velocity $\mathbf{\Delta V}$ vector.

As shown in Fig. 2, A represents an underwater vehicle and B represents a moving obstacle in the space. In order to better analyze the motion relationship between the underwater vehicle and the obstacle, the size of the underwater vehicle is superimposed on the size of the moving obstacle. sd is used to represent the radius of the moving obstacle that has been processed. S is the distance between the underwater vehicle and the moving obstacle at current time. The angle between the segment AB and the tangent of the expanding circle is called the collision angle μ, $\mu = arcsin(sd/S)$, γ is the angle between the current relative velocity and the current position line. When γ is greater than μ , the underwater vehicle is safe in the current state of motion, as long as the motion state does not change. Otherwise, there is a possibility of collisions between the underwater vehicle and the moving obstacle. Take the underwater vehicle A as the center of the circle, the sectorial regions consisted of tangents A and B are defined as "collision zones", which may be dangerous.

When performing collision prediction analysis of the underwater vehicle and the obstacle, we can do the corresponding direction decomposition for their respective velocities in the direction of AB and in the direction perpendicular of AB.

$$\begin{cases} \mathbf{V}_S = \mathbf{V}_A\cos(\alpha-\theta) - \mathbf{V}_B\cos(\beta-\theta) \\ \mathbf{V}_\theta = \mathbf{V}_A\sin(\alpha-\theta) - \mathbf{V}_B\sin(\beta-\theta) \end{cases} \quad (25)$$

$\mathbf{V}_S$ is the relative velocity component in the AB direction. $\mathbf{V}_\theta$ is the relative velocity component in the vertical direction of AB. As shown in Fig. 3, $\Delta\mathbf{V}$ is the relative velocity of the underwater vehicle A relative to the obstacle B. α is the angle between the sailing velocity $\mathbf{V}_A$ of the underwater vehicle and the x coordinate axis. β is the angle between the velocity $\mathbf{V_B}$ of the obstacle and the x coordinate axis. θ is the angle between the line AB connecting the underwater vehicle and the moving obstacle and the x coordinate axis.

B. AUV Collision Avoidance Strategy

When there is a possibility of a collision between the underwater vehicle and the moving obstacle, the underwater vehicle needs urgent avoidance adjustment. The adjustment of collision avoidance is mainly performed by adjusting the velocity of the underwater vehicle. The angle γ between the relative velocity and the line AB is greater than safety angle μ through the emergency collision avoidance adjustment. According to Eq. (13):

$$\tan\gamma = \frac{\mathbf{V}_\theta}{\mathbf{V}_S} = \frac{\mathbf{V}_A\sin(\alpha-\theta) - \mathbf{V}_B\sin(\beta-\theta)}{\mathbf{V}_A\cos(\alpha-\theta) - \mathbf{V}_B\cos(\beta-\theta)} \quad (26)$$

A function of velocity between the underwater vehicle and the moving obstacle is constructed below.

$$f(\mathbf{V}_A, \alpha, \mathbf{V}_B, \beta) = \tan\gamma \quad (27)$$

then

$$\gamma = arc\tan f(\mathbf{V}_A, \alpha, \mathbf{V}_B, \beta) \quad (28)$$

$$\begin{aligned} d\gamma &= \tfrac{1}{1+f^2}df \\ &= \tfrac{[\mathbf{V}_B\cos(\beta-\theta) - \mathbf{V}_A\cos(\alpha-\theta)]^2}{\mathbf{V}_A^2 + \mathbf{V}_B^2 - 2\mathbf{V}_A\mathbf{V}_B\cos(\alpha-\beta)}df \end{aligned} \quad (29)$$

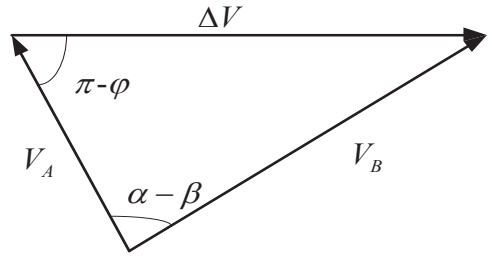

Fig. 4. Velocity relation diagram

$$df = \frac{\partial f}{\partial \mathbf{V}_A} d\mathbf{V}_A + \frac{\partial f}{\partial \alpha} d\alpha + \frac{\partial f}{\partial \mathbf{V}_B} d\mathbf{V}_B + \frac{\partial f}{\partial \beta} d\beta \quad (30)$$

Because of the fact that only the speed of the underwater vehicle can be controlled by man during the course of movement, the movement state of the moving obstacle cannot be adjusted artificially. While the underwater vehicle adjusting the velocity, it is assumed that the moving obstacle still maintains the original motion modewhich means that the velocity of the obstacle doesn't change in this time. According to Eq. (18):

$$\begin{aligned} df &= \tfrac{\partial f}{\partial \mathbf{V}_A} d\mathbf{V}_A + \tfrac{\partial f}{\partial \alpha} d\alpha = d\bar{\mathbf{V}}_A \\ &= \tfrac{-\mathbf{V}_B \sin(\alpha-\beta)}{[\mathbf{V}_B \cos(\beta-\theta) - \mathbf{V}_A \cos(\alpha-\theta)]^2} d\mathbf{V}_A \\ &+ \tfrac{\mathbf{V}_A[\mathbf{V}_A - \mathbf{V}_B \cos(\alpha-\beta)]}{[\mathbf{V}_B \cos(\beta-\theta) - \mathbf{V}_A \cos(\alpha-\theta)]^2} d\alpha \end{aligned} \quad (31)$$

So the Eq. (17) can be written as follows:

$$\begin{aligned} d\gamma = &\tfrac{-\mathbf{V}_B \sin(\alpha-\beta) d\mathbf{V}_A +}{\mathbf{V}_A^2 + \mathbf{V}_B^2 - 2\mathbf{V}_A \mathbf{V}_B \cos(\alpha-\beta)} \\ &+ \tfrac{\mathbf{V}_A[\mathbf{V}_A - \mathbf{V}_B \cos(\alpha-\beta)] d\alpha}{\mathbf{V}_A^2 + \mathbf{V}_B^2 - 2\mathbf{V}_A \mathbf{V}_B \cos(\alpha-\beta)} \end{aligned} \quad (32)$$

The approximate solution of the above formula is obtained using the difference method:

$$\begin{aligned} \Delta\gamma = &\tfrac{-\mathbf{V}_B \sin(\alpha-\beta) \Delta\mathbf{V}_A}{\mathbf{V}_A^2 + \mathbf{V}_B^2 - 2\mathbf{V}_A \mathbf{V}_B \cos(\alpha-\beta)} \\ &+ \tfrac{\mathbf{V}_A[\mathbf{V}_A - \mathbf{V}_B \cos(\alpha-\beta)] \Delta\alpha}{\mathbf{V}_A^2 + \mathbf{V}_B^2 - 2\mathbf{V}_A \mathbf{V}_B \cos(\alpha-\beta)} \end{aligned} \quad (33)$$

As we can seen from Fig. 4

$$\mathbf{V}_B \sin(\alpha - \beta) = \Delta\mathbf{V} \sin\varphi \quad (34)$$

$$\mathbf{V}_A - \mathbf{V}_B \cos(\alpha - \beta) = -\Delta\mathbf{V} \cos\varphi \quad (35)$$

$$\mathbf{V}_A^2 + \mathbf{V}_B^2 - 2\mathbf{V}_A \mathbf{V}_B \cos(\alpha - \beta) = \Delta\mathbf{V}^2 \quad (36)$$

then

$$\Delta\gamma = \frac{1}{\Delta\mathbf{V}}(-\Delta\mathbf{V}_A \sin\varphi - \mathbf{V}_A \Delta\alpha \cos\varphi) \quad (37)$$

and

$$V_A \Delta\alpha = -(\tan\varphi \Delta V_A + \Delta V \Delta\gamma / \cos\varphi) \quad (38)$$

As shown in Fig. 5, the acceleration space coordinates is obtained according to Eq.(26). From Fig. 2 and Fig. 5, l is the line of relative velocity of the underwater vehicle relative to the obstacle. The adjustable range of $\Delta\gamma$ is a band with a width of $2u$, i.e., $\Delta\gamma = u - \gamma$ and $\Delta\gamma = u - \gamma$. This zone is a collision zone, so we need to adjust the velocity and the course of the underwater vehicle so that leaving the collision zone as soon as possible.

Suppose that the control regulation of the underwater vehicle is fixed. For the AUV velocity control, obstacles can only be treated at reduced speed in the full speed navigation.

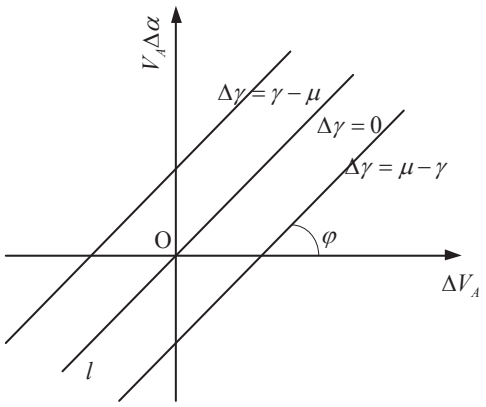

Fig. 5. Acceleration space coordinates

In order to adjust the velocity of the AUV, a force will be exerted on it so as to get an acceleration. Suppose that the regulation of acceleration can be divided into five stalls: $-0.1m/s^2$, $-0.2m/s^2$, $-0.3m/s^2$, $-0.4m/s^2$, $-0.5m/s^2$. Accordingly, give the acceleration control weights p to the five stalls, they are 1, 2, 3, 4 and 5, respectively. In terms of AUV heading adjustment, the angular acceleration obtained by applying an external force is also divided into five stalls: $0.1rand/s^2$, $0.2rand/s^2$, $0.3rand/s^2$, $0.4rand/s^2$, $0.5rand/s^2$. Accordingly, the angular acceleration control weight is also assigned to each stall, which are 1, 2, 3, 4 and 5, respectively. In this way, the control problem is transformed into an integer linear programming problem. Let the control time be 1s, then for each weight, there is a corresponding change in velocity or angular velocity.

Whenever obstacle avoidance control is required, under the minimum weight, the $T = p+q$ can be minimized, so that the angle γ is greater than the security angle μ. When multiple processing methods are used with equal weight, select the control combinations that maximize γ after processing. If multiple obstacles exist in the planning space, computing the minimum weight control combinations that can successfully avoid all obstacles. Thus, the obstacle avoidance strategy selection process is transformed into solving an integer linear programming problem. The obstacle avoidance strategy can accomplish the obstacle avoidance process with minimal changes to the AUV.

IV. Obstacle Avoidance Simulation Experiment for AUV

Extended Kalman filter is used to predict the trajectory of dynamic obstacle. As shown in Fig. 6, the position error is relatively stable, and it is controlled within 0.5 meters. The motion trajectory is consistent with the real trajectory, which proves the validity and accuracy of the mathematical model in Fig. 7.

In the simulation of collision avoidance, the initial position of the underwater vehicle is at (0,0) point. The heading moves at a speed of $2m/s$ along the X axis. No.1 obstacle is a circular area with a radius of 10m, and the initial position is at (40,100) point. The obstacle moves at a constant velocity along X and Y directions. The velocity is $1.5m/s$ along X direction, and $-2m/s$ along Y direction. No.2 obstacle is static and located at point (150,0) in the coordinate system. No.2 obstacle is also a circular area with a radius of 10m.

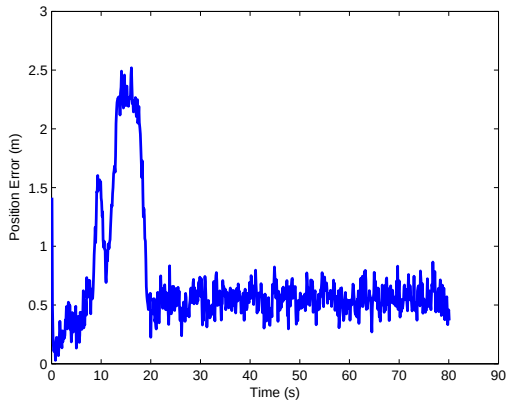

Fig. 6. The positioning error

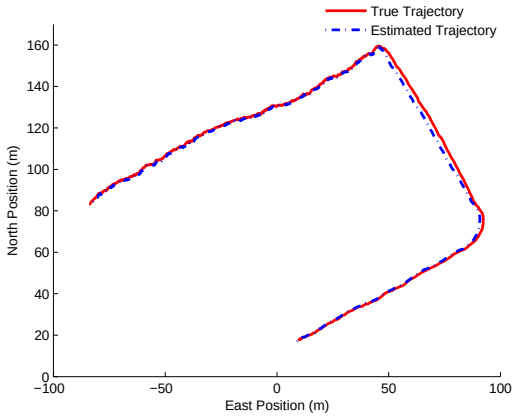

Fig. 7. Trajectory of dynamic obstacles

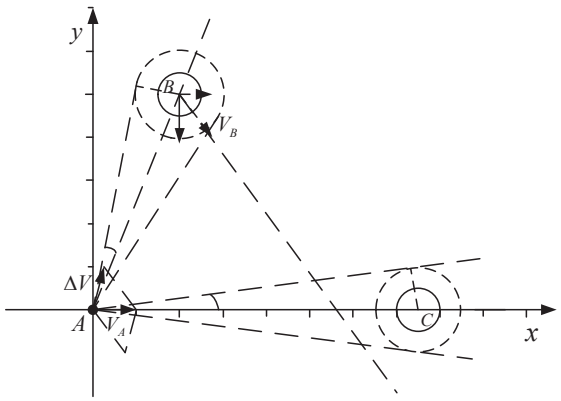

Fig. 8. Initial state diagram of motion space

Let the safety distance of the AUV be 10 meters. First, the security distance is superposed on the moving obstacle, and the initial state as shown in Fig. 8 is obtained. In Fig. 8, A stands for the AUV, B stands for No.1 obstacle, C stands for No.2 obstacle, $\mathbf{V_A}$ is the sailing velocity of the AUV, $\mathbf{V_B}$ is the velocity of No.1 obstacle, $\mathbf{\Delta V}$ is the relative velocity between the AUV and No.1 obstacle.

From the initial state, if the underwater vehicle travels at its original course and speed, it will collide with obstacle C. The underwater vehicle will also collide with the obstacles B, because the relative velocity is in the collision zone of the obstacles B. Therefore, collision avoidance must be carried

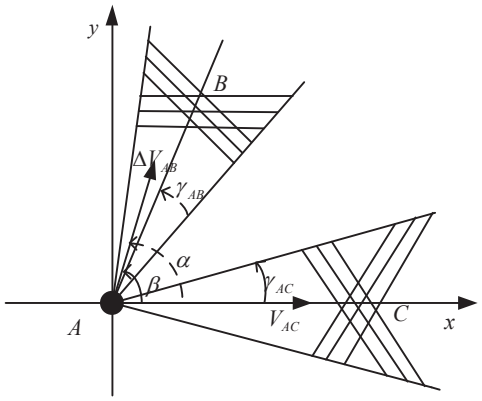

Fig. 9. AUV avoidance control diagram

TABLE I
COLLISION AVOIDANCE RESULTS OF OBSTACLE B

Collision Avoidance Processing	L 0	L 1	L 2	L 3	L 4	L 5	R 0	R 1	R 2	R 3	R 4	R 5
Retard 0	0	0	0	1	1	1	0	0	0	0	0	0
Retard 1	0	0	1	1	1	1	0	0	0	0	0	0
Retard 2	1	1	1	1	1	1	0	0	0	0	0	0
Retard 3	1	1	1	1	1	1	0	0	0	0	0	0
Retard 4	1	1	1	1	1	1	0	0	0	0	0	0
Retard 5	1	1	1	1	1	1	0	0	0	0	0	0

TABLE II
COLLISION AVOIDANCE RESULTS OF OBSTACLE C

Collision Avoidance Processing	L 0	L 1	L 2	L 3	L 4	L 5	R 0	R 1	R 2	R 3	R 4	R 5
Retard 0	0	0	0	1	1	1	0	0	0	1	1	1
Retard 1	0	0	0	1	1	1	0	0	0	1	1	1
Retard 2	0	0	0	1	1	1	0	0	0	1	1	1
Retard 3	0	0	0	1	1	1	0	0	0	1	1	1
Retard 4	0	0	0	1	1	1	0	0	0	1	1	1
Retard 5	0	0	0	1	1	1	0	0	0	1	1	1

out for the AUV. For the obstacle B, $\mathbf{\Delta V_{AB}}$ must deviate from the collision zone of the obstacle B, and $\mathbf{\Delta V_{AC}}$ must also deviate from the collision zone of the obstacle C. AUV avoidance control diagram is shown in Fig. 9.

According to the weight control defined in the previous section, the control results of collision avoidance for two obstacles can be obtained, which are shown in Table I and Table II, respectively, where in L stands for left, and R stands for right. In order to verify the effectiveness of the method, we increase another experiment, the initial position of underwater vehicle is at (10,6). The heading move at a speed of $3m/s$ along the X axis. No.1 obstacle is a circular area with a radius of $20m$, and the initial position is at (140,200) point. The obstacle moves at a constant velocity along X and Y directions. The velocity is $2.5m/s$ along X direction, and $-2.8m/s$ along Y direction. No.2 obstacle was static and located at point (190,0) in the coordinate system . the control results of collision avoidance for two obstacles could be obtained, which were shown in Table III and Table IV, respectively.

Left and right in the table represent the yaw control direction, i.e., the angular acceleration direction. 0 indicates that combination obstacle avoidance control is unsuccessful.

TABLE III
COLLISION AVOIDANCE RESULTS OF OBSTACLE B

Collision Avoidance Processing	L 0	L 1	L 2	L 3	L 4	L 5	R 0	R 1	R 2	R 3	R 4	R 5
Retard 0	0	0	1	1	1	0	1	0	0	0	1	0
Retard 1	0	0	0	0	1	0	1	0	0	0	0	0
Retard 2	1	1	1	1	1	0	1	0	0	0	0	0
Retard 3	1	1	0	1	1	0	1	0	0	0	1	0
Retard 4	1	1	1	0	1	0	1	0	0	0	0	0
Retard 5	1	1	1	1	1	0	1	0	0	0	0	0

TABLE IV
COLLISION AVOIDANCE RESULTS OF OBSTACLE C

Collision Avoidance Processing	L 0	L 1	L 2	L 3	L 4	L 5	R 0	R 1	R 2	R 3	R 4	R 5
Retard 0	1	0	0	1	0	0	0	0	1	1	0	1
Retard 1	0	0	0	1	0	1	0	0	1	0	0	1
Retard 2	1	0	0	1	1	0	0	0	1	1	0	1
Retard 3	0	0	0	1	0	1	0	0	1	0	0	1
Retard 4	1	0	0	1	1	1	0	0	0	1	0	1
Retard 5	0	0	0	1	1	0	0	0	1	0	0	1

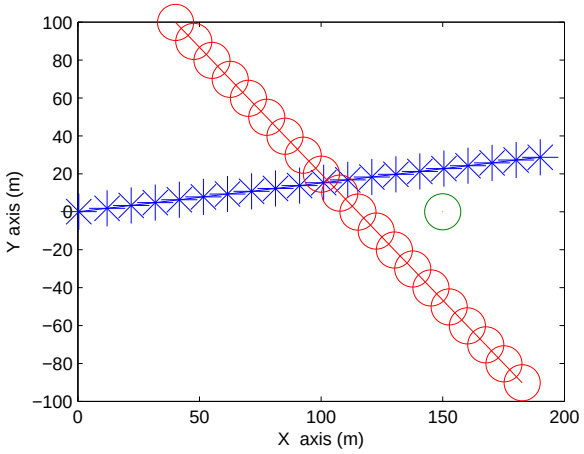

Fig. 10. Location diagram during obstacle avoidance

1 indicates that combination obstacle avoidance control is successful. The result shows that obstacle avoidance control combination with minimum weight through overall consideration, is angular acceleration left yaw control 3, acceleration control 0, the weight is 3. After this operation, AUV can successfully avoid the threat from the obstacle. The spatial distribution of the underwater vehicle and the obstacle varies with time is shown in Fig. 10.

As can be seen from Eq.(26), the velocity and direction adjustment of the underwater vehicle, $\mathbf{\Delta V_A}$ and $\Delta\alpha$ are related to $\Delta\gamma$. In each discrete time T, the obstacle is avoided through real-time adjustment of $\Delta\alpha$ and $\mathbf{\Delta V_A}$. $\Delta\alpha$ is the variation of velocity direction. $\mathbf{\Delta V_A}$ is the variation of velocity size, i.e., acceleration. $\mathbf{\Delta V}$ is the variation of relative velocity, i.e., relative acceleration. In other words, $\mathbf{\Delta V_A}$ is the acceleration component along the $\mathbf{V_A}$ direction. $\mathbf{V_A}\Delta\alpha$ is approximated as an acceleration component perpendicular to the velocity direction of the AUV. According to the above theory, the simulation results are shown as follows.

Fig. 11 shows the velocity change in the cycle of AUV performing obstacle avoidance and controls. Fig. 12 shows

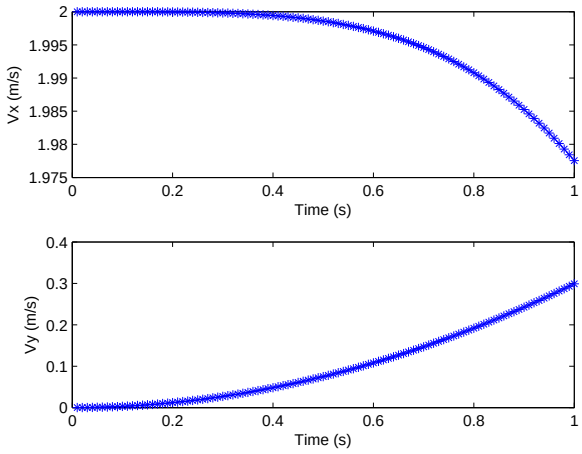

Fig. 11. AUV velocity change diagram

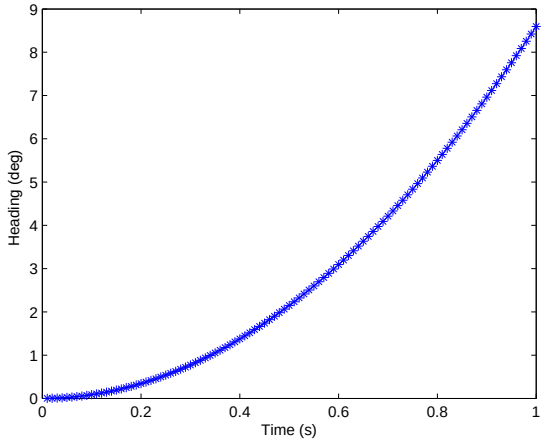

Fig. 12. AUV course change diagram

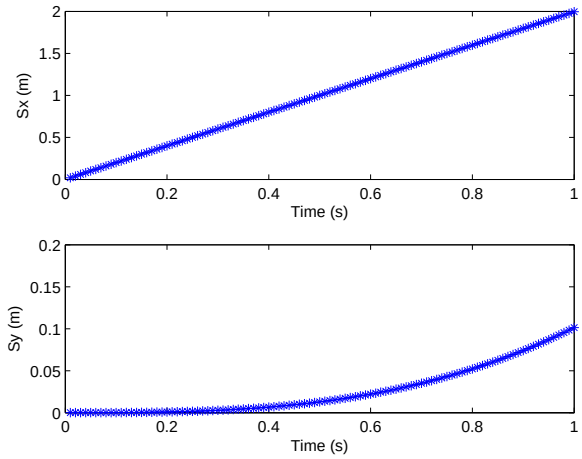

Fig. 13. AUV displacement change diagram

the course change of underwater vehicle in the cycle of obstacle avoidance and controls. The underwater vehicle controls the relative velocity by adjusting its velocity to achieve the obstacle avoidance effect. Fig. 13 shows the displacement change of the underwater vehicle during the obstacle avoidance period. Fig. 10 shows the trajectory of the underwater vehicle and the obstacle in space. As shown in Fig. 10, through the previous obstacle avoidance processing, the underwater vehicle could successfully avoid the threat of the obstacle.

V. Conclusion

The real-time path planning of underwater vehicle in dynamic obstacle environment is presented in this paper. A mathematical model of dynamic obstacle is established to predict the trajectory of vehicle. To determine whether there is a collision will occur by evaluating the speed of relative movement of the vehicle and obstacles. And finally adopt strategies against for some threatens to avoid collision. The simulation experiment of the algorithm shows that the predicted trajectory is accurate and effective, and the reaction strategy enables the vehicle to successfully avoid moving obstacles and finally achieve collision avoidance.

References

[1] S. S. Ge and Y. J. Cui, "Dynamic Motion Planning for Mobile Robots Using Potential Field Method," *Autonomous Robots*, vol. 13, no. 3, pp. 207-222, 2002.

[2] F. Large, S. Sekhavat and Z. Shiller, "Towards real-time global motion planning in a dynamic environment using the NLVO concept[C]," *International Conference on Intelligent Robots and Systems IEEE*, 1 (2002) 607-612.

[3] I. Ulrich and J. Borenstein, "VFH*: Local obstacle avoidance with look-ahead verification[C]," *International Conference on Robotics and Automation IEEE*, 3 (2000) 2505-2511.

[4] J. L. Fernndez, R. Sanz and J. A. Benayas, "Improving collision avoidance for mobile robots in partially known environments: the beam curvature method," *Robotics and Autonomous Systems*, vol. 46, no. 4, pp. 205-219, 2004.

[5] H. J. XIE and H. Z. WANG, "Dynamic collision avoidance planning for mobile robot based on velocity resolution," *Journal of East China University of Science and Technology*, vol. 37, no. 2, pp. 234-238, 2011.

[6] B. Friedland, "Optimum Steady-State Position and Velocity Estimation Using Noisy Sampled Position Data," *IEEE Transactions on Aerospace Electronic Systems*, vol. 9, no. 6, pp. 906-911, 1973.

[7] P. Bigaj and J. Bartoszek, "Low Time Complexity Collision Avoidance Method for Autonomous Mobile Robots," in *Intelligent Systems'2014. Springer International Publishing*, pp. 141-152, 2015.

[8] L. Zeng and G. M. Bone, "Mobile Robot Collision Avoidance in Human Environments," *International Journal of Advanced Robotic Systems*, vol. 10, no. 41, pp. 257-271, 2013.

[9] F. Liccardo, S. Strano and M. Terzo, "Real-time nonlinear optimal control of a hydraulic actuator," *Engineering Letters*, vol. 21, no. 4, pp. 241-246, 2013.

[10] A. Nattapol, "A bayesian filtering approach with time-frequency representation for corrupted dual tone multi frequency identification," *Engineering Letters*, vol. 24, no. 4, pp. 370-377, 2016.

[11] F. Srairi, L. Saidi, F. Djeffal and M. Meguellati, "Modeling, control and optimization of a new swimming microrobot design," *Engineering Letters*, vol. 24, no. 1, pp. 106-112, 2016.

[12] C. H. Yu and J. W. Choi, "Interacting multiple model filter-based distributed target tracking algorithm in underwater wireless sensor networks," *International Journal of Control Automation and Systems*, vol. 12, no. 3, pp. 618-627, 2014.

[13] A. Sebastian, G. Gerardo, L. Andre and A. Rozenfel, "Evaluation of an efficient approach for target tracking from acoustic imagery for the perception system of an autonomous underwater vehicle," *International Journal Of Advanced Robotic Systems*, vol. 11, no. 1, pp. 1, 2014.

[14] F. Tajti and M. Burdelis, "A novel potential field method for path planning of mobile robots by adapting animal motion attributes," *Robotics and Autonomous Systems*, vol. 82, pp. 23-34, 2016.

[15] D. Q. Zhu, C. L. Cheng and B. Sun, "An integrated AUV path planning algorithm with ocean current and dynamic obstacles," *International Journal of Robotics and Automation*, vol. 31, no. 5, pp. 382-389, 2016.